Full Paper

Wiley Online Library

ELECTROANALYSIS

DOI: 10.1002/elan.201900141

Enhanced Electrocatalytic Oxidation of Paracetamol at DNA Modified Gold Electrode

Ismail I. Althagafi,[a] Mohammed A. Kassem,*[a, b] and Mohamed I. Awad*[a, c]

Abstract: Cysteine monolayer has been assembled onto bare gold electrode (SAM/Au), and subsequently deoxyribonucleic acid (DNA) has been successfully immobilized at the SAM/Au electrode. The thus modified electrode is assigned DNA/SAM/Au. Modification steps of the electrode were followed electrochemically using $K_4[Fe(CN_6)]$ electrochemical marker. Also, the build-up of the modified electrode composition is followed using EDX and the crystallographic orientation is inspected using XRD. The electrochemical behavior of paracetamol (PC) at DNA/SAM/Au electrode is investigated. Interestingly, the sluggish irreversible behavior of PC at the bare gold electrode is converted to a quasi-reversible one at DNA/SAM/Au electrode pointing to some interaction between the immobilized DNA and PC. The enhanced electrochemical behavior of PC at modified DNA/SAM/Au electrode is successfully used for a sensitive electrochemical determination of PC. Square wave voltammetry (SWV) was used for this purpose. The concentration of PC was in linear relation with the peak current at the optimum conditions within the range 10.0–110.0 $\mu g\,mL^{-1}$ with correlation coefficient (R^2) of 0.998. Also, the standard deviation (SD) and relative standard deviation (RSD) were calculated and found to be 0.817 and 1.52, respectively, indicating the significance of the present method.

Keywords: Self-assembly monolayer · DNA · Paracetamol · Electrocatalysis

1 Introduction

Deoxyribonucleic acid (DNA) is the information source controlling all life processes of the organism. Transcription and replication, which are the main functions of the DNA, are vital to functioning of all body processes in the proper way. DNA interactions with drugs have become an active area of research as DNA is the major target of drug interactions. These interactions have been utilized as a base for the estimation of DNA and/or drugs [1–3]. Such interactions are a fundamental issue in life process, for gene delivery systems. On the other hand, analytical determination based on DNA is an essential for clinical diagnosis in discovering the different ways which develop the disease, and consequently to find suitable ways of remediation. Several analytical methods have been reported, as for instance, flow injection chemiluminescence, capillary electrophoresis, ion pairing liquid, micellar electrokinetic chromatography and laser-induced fluorescence detection [4–10]. Also, interactions of DNA with some drugs have been utilized in the analysis of these drugs at DNA modified electrodes. For instance, the analysis of didanosine [11] and 6-mercaptopurine [12] using voltammetric techniques, which are sensitive, simple and compatible with micro fabrication technology. It offers advantages over conventional used biological and chemical assays. Signal amplification strategies have been used to increase the electrochemical biosensors sensitivity. In this correspondence, electro-active polymer as the transduction element has been reported [13–21]. The electroactivity of DNA at those electrodes is controlled by the structure and conformation of DNA as well as its damage [18,19]. Electroactivity of DNA is due to the presence of adenine, cytosine and guanine [22,13–20]. In the present work, the DNA modified gold electrode is utilized in the enhanced electrocatalytic oxidation and the subsequent electroanalysis of paracetamol (PC). PC is a main component in plentiful cold and flu medications. It is widely used over-the-counter analgesic and antipyretic for the relief of headaches and other minor pains. A rapid simple method for the analysis of PC is needed for pharmaceutical control. Several methods have been reported for assaying PC in pharmaceutical preparations [23–31]. Among these methods, chromatographic methods

[a] I. I. Althagafi, M. A. Kassem, M. I. Awad
Chemistry Department, Faculty of Applied Science, Umm Al-Qura University, Makkah, Kingdom Saudi Arabia
Tel: 00966595491550
E-mail: mawad70@yahoo.com
miawad@uqu.edu.sa

[b] M. A. Kassem
Chemistry Department, Faculty of Science, Benha University, Benha, 13518, Egypt
Tel: 00966532175442
E-mail: maa_kassem@hotmail.com
makassem@uqu.edu.sa

[c] M. I. Awad
Chemistry Department, Faculty of Science, Cairo University, Cairo, Egypt
E-mail: mawad70@yahoo.com
miawad@uqu.edu.sa

Supporting information for this article is available on the WWW under https://doi.org/10.1002/elan.201900141

are the most common for the determination of PC and has been recommended by the American Pharmacopoeia as the official method [32]. However, these methods are time consuming and need tedious sample pretreatment. Electrochemical determination at glassy carbon, gold and platinum modified electrodes for PC either individually or the coexistence with some other drugs, has been reported [23–27]. Among these modifications, derivatization of gold nanoparticles by thiol has deserved as a base modification of the thus modified electrode with DNA [33–41]. Thus, the present research is devoted for the utilization of the interaction of DNA assembled on a transducer, as a base for the electroanalysis of PC. Immobilizing DNA at an electrode is the controlling step in fabrication of a DNA modified electrode as the immobilized extent control its suitability. Cysteine is used in the present work to enhance the assembling of DNA, and subsequently the electrochemical behavior of PC at the DNA modified electrode is investigated and used as a base for its analytical determination. The present method offers a simple voltammetric analysis of PC over a suitable rectilinear range.

2 Experimental

2.1 Reagents and Chemicals

L-cysteine ($C_3H_7NO_2S$), Cys, potassium ferrocyanide ($K_4[Fe(CN)_6]$) and sulfuric acid were obtained from Sigma-Aldrich and used as received without further purification. Potassium hydroxide (KOH) was obtained from Riedel Company. A series of phosphate buffer solutions (PBs) with different pHs were prepared according to Gomari [42]. A 0.05 M H_2SO_4 was prepared by accurate dilution using bidistilled water. A stock of 200 $\mu g\,mL^{-1}$ PC (obtained as a gift from Amriya Pharmaceutical Industries, Alexandria, Egypt) was prepared by dissolving accurately 20 mg PC in 100 mL bidistilled water. Calf thymus DNA-sodium salt (from Sigma-Aldrich: CAS. 73049-39-5) was prepared as described in literature [43]. Once dissolved, the DNA solution is sheared to an average size of $\leq$2000 bp. Its concentration and purity were determined spectrophotometrically by calculating the ratio of its absorbance at 260 and 280 nm. The ratio A_{260}/A_{280} was around 1.8 indicating an acceptable purity of the prepared DNA.

2.2 Electrodes

The polycrystalline gold (poly–Au) was polished with fine alumina powder, rinsed with water and then was subjected to sonication for removal of the remaining alumina particles. The Au electrode was then electrochemically pretreated in N_2-saturated 0.05 M sulfuric acid solution until the characteristic CV for clean Au electrode was obtained.

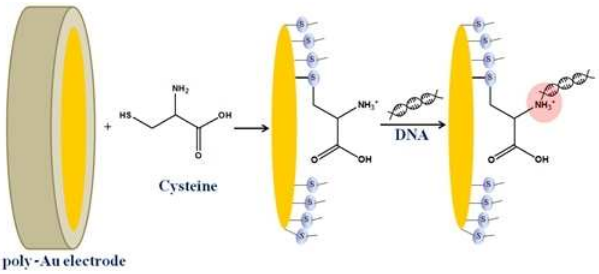

Scheme 1. Schematic representation of anchoring DNA onto SAM/Au electrode.

2.3 Preparation of the Modified Electrode

Scheme 1 shows the steps of the preparation of the DNA anchored onto self-assembly modified gold electrode (DNA/SAM/Au). Firstly, a full monolayer of cysteine was self-assembled onto the poly–Au electrode by soaking the clean gold electrode into a freshly prepared aqueous solution of 1.0 mM cysteine for 20 min and then washed with aliquots of distilled water to remove the physically adsorbed cysteine. The prepared electrode is assigned SAM/Au. Subsequently DNA is casted on SAM/Au and left for drying for 2 hours to obtain the modified sensor assigned as DNA/SAM/Au. Direct modification of gold electrode with DNA is not stable, so gold electrode was modified with cysteine (Cys/Au) at first. As it is well known that the bond formed between thiol and gold is very strong [44,45], then DNA subsequently modified onto Cys/Au electrode utilizing the possible electrostatic interaction between the cysteine and the negatively charged DNA.

2.4 Measurements

Electrochemical measurements were conducted using PGSTAT30 potentiostat/galvanostat. An Ag/AgCl (KCl sat.) electrode was used as the reference electrode. A platinum spiral wire was used as a counter electrode. A conventional three-electrode cell of about 40 mL volume was used. All electrochemical measurements were conducted under nitrogen saturated solutions. The optimum parameters used in the measurement were SW amplitude of 20 mV, frequency at 50 Hz and the step height of 5 mV. All voltammetric experiments were repeated at least three times to check the repeatability and for calculating the standard deviations. Jeol JSM 6400 system were used for EDX spectra. The electron energy used was 20 keV. XRD measurements were performed using Philips PW 1700 powder X-ray diffractometer using Cu Ka1 radiation with a Ni filter working at 40 kV and 30 mA.

3 Results and Discussion

3.1 Surface Characterization

DNA anchored onto self-assembly modified gold (DNA/SAM/Au) electrode composition was probed using energy dispersive X-ray (EDX) analysis and compared with bare gold electrode (Au) and cysteine modified gold electrode (SAM/Au) and results are shown in Figure 1A. The signals which correspond to gold atoms, c.a. 2.4 (the main peak), 11.2 and 9.8 Kev, are clearly observed in the case of bare Au and SAM/Au electrodes. In the case of DNA/SAM/Au electrode, the peak at around 2.4 KeV are suppressed [46]. In addition, a new peak, for nitrogen, at around 0.4 is clearly shown. The latter peak is most likely belonging to the constituents of DNA. These confirm the successful assembling of DNA.

Crystallographic orientation of the gold facets was propped using XRD as shown in Figure 1B. Bragg reflection main peak revealed at 38° corresponds to (111) facet along with some other peaks at 78°, 82°, 85° and 88° corresponds to (311). The peaks at 38° and 78° correspond to standard Bragg reflections of face centres cubic (JCPDS File No. 00-001-1174) [46]. The peak at 78° (311) is suppressed in the case of DNA/SAM/Au electrode. This again confirms the successful modification of the DNA onto SAM/Au electrode. In addition, it points to preferential deposition on some facets of the poly–Au electrode.

3.2 Electrochemical Characterization

The bare Au electrode used as a substrate for the further assembling of cysteine and DNA is electrochemically characterized by $K_4[Fe(CN)_6]$ electrochemical marker. Figure 2 shows cyclic voltammograms for $K_4[Fe(CN)_6]$ obtained at (a) bare Au, (b) SAM/Au, (c) DNA/Au and (d) DNA/SAM/Au electrodes prepared as mentioned in the experimental section. The parameters obtained from this figure are shown in Table 1S. The well-defined redox couple for $K_4[Fe(CN)_6]$ is obtained for all the studied electrodes. In the case of bare Au electrode (curve a), the separation between anodic and cathodic peak potentials was $\simeq$95 mV. In the case of SAM/Au electrode (curve b), the potential couple is negatively shifted. In addition, the peak current is increased, probably due to some interaction between the assembled cysteine molecules and ferricyanide. The separation between the potential of the two peaks is the smallest among studied electrodes indicating the electron and mass transfer enhancement. On the contrary, in the case of DNA/Au (curve c) electrode, the potential couple is positively shifted as a result of the repulsion between the $K_4[Fe(CN)_6]$ and the phosphate group in DNA [47]. In addition, the peak current is decreased. This decrease might denote the change in the diffusion of $K_4[Fe(CN)_6]$ and consequently retardation in the mass transfer. In the case of DNA/SAM/Au electrode (curve d), still the peak current is larger than that obtained at the bare Au electrode.

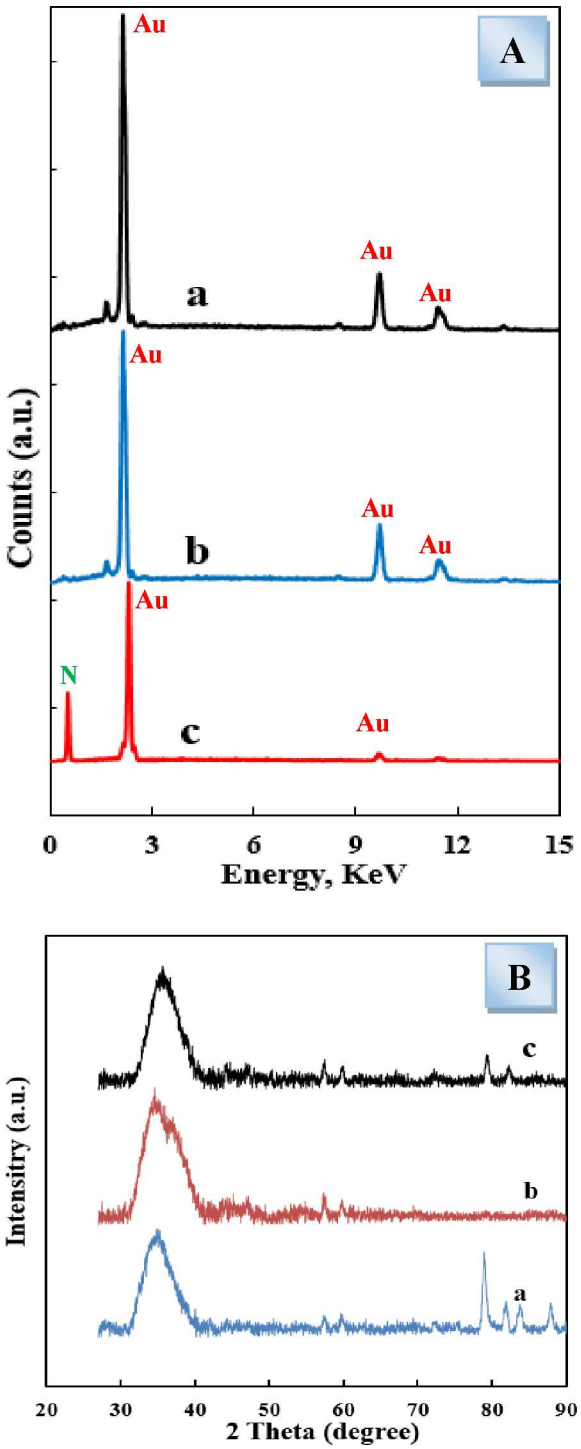

Fig. 1. **A**) EDX analysis for (a) bare Au, (b) SAM/Au and (c) DNA/SAM/Au electrodes, **B**) XRD analysis for (a) bare Au, (b) SAM/Au and (c) DNA/SAM/Au electrodes.

However, the enhancement obtained at SAM/Au is decreased after the immobilization of DNA denoting the successful binding of DNA to the cysteine modified gold electrode. The change in the separation between peak potentials indicates the stable modification of DNA at the cysteine modified electrode, as compared with the direct

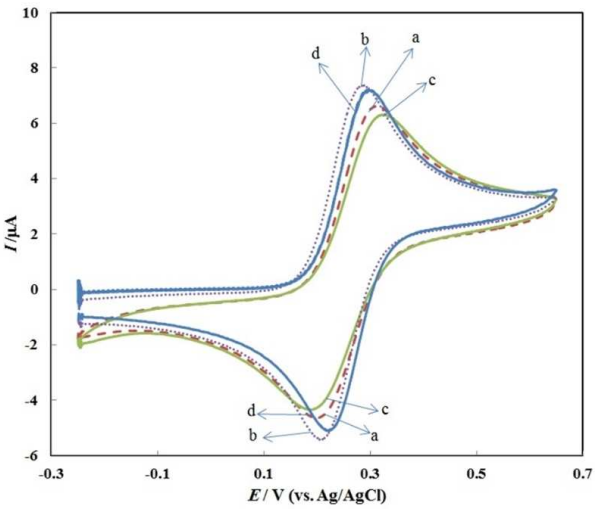

Fig. 2. Cyclic voltammograms for $K_4[Fe(CN)_6]$ obtained at (a) Au, (b) SAM/Au, (c) DNA/Au and (d) DNA/SAM/Au electrodes, Scan rate is 100 mV/s.

assembling of DNA at bare Au electrode, as schematically represented in Scheme 1 shown above.

Next, the electrochemical behavior of PC at the studied electrodes was examined. Figure 3 shows cyclic voltammograms obtained for 53 µM paracetamol at those electrodes. Electrochemical parameters extracted from this figure are shown as Table 2S. In the case of bare Au electrode (curve a), well defined anodic and cathodic peaks for the oxidation and the coupled reduction of PC

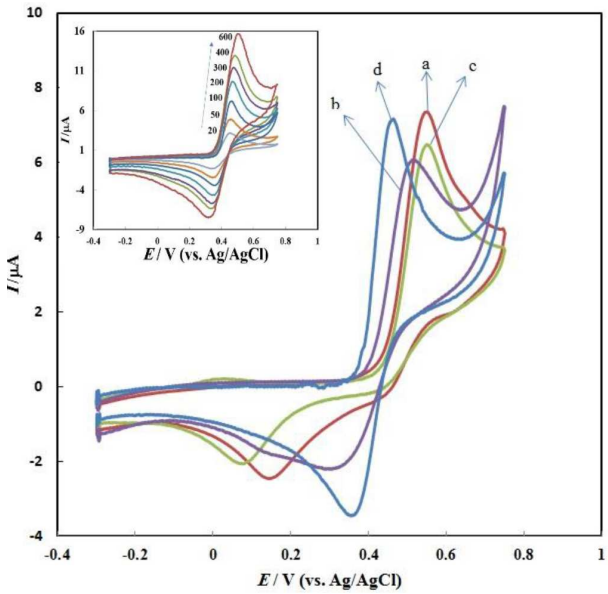

Fig. 3. CV obtained for 0.053 mM paracetamol obtained at (a) Au, (b) SAM/Au, (c) DNA/Au and (d) DNA/SAM/Au electrodes at scan rate of 100 mV/s. (Inset, Effect of scan rate) (Numbers in figure are in mV/s).

are obtained at ca. 0.56 and 0.15 V, respectively. This redox couple can be represented by equation 1.

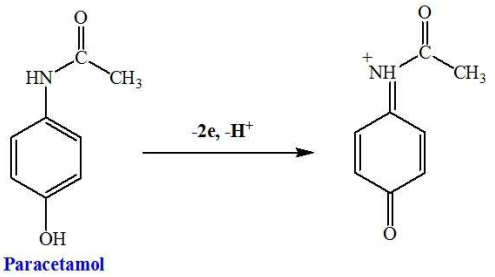

(1)

The large peak potential separation reveals the irreversible nature of PC redox behavior at bare Au electrode. At SAM/Au (curve b) electrode, an anodic peak is obtained at around 0.51 V, i.e., at lower positive potential with respect to poly–Au electrode. This anodic peak is coupled with two cathodic peaks at 0.14 and 0.33 V, respectively. The cathodic peak obtained at 0.14 V is at the same potential similar to that obtained at bare Au electrode. It might belong to the reduction at the cysteine-uncovered portion of the electrode. At DNA/Au (curve c) electrode, the potential of the anodic peak, 0.56 V, does not change compared with bare Au electrode. However, the peak current slightly decreased probably due to the poor direct assembling of DNA onto unmodified gold electrode. The cathodic peak is more than 100 mV cathodically shifted pointing to the suppressing of the cathodic reduction in this case. At DNA/SAM/Au (curve d) electrode, interestingly, the electrode kinetics is largely enhanced; the anodic peak is 100 mV negatively shifted and the cathodic peak is 300 mV positively shifted. The separation between peak potential in the present case is around 90 mV. In addition, the ratio of the anodic peak current with respect to the cathodic peak current is the smallest, c.a., 1.46. Table 2S.

The sluggish kinetics obtained at bare Au electrode is changed to quasi-reversible one at DNA/SAM/Au electrode, as revealed from the effect of scan rate on the peak current (Figure 3, Inset). As the scan rate increases the separation between the anodic and cathodic peaks increases indicating a quasi-reversible process. The smallest peak separation obtained at DNA/SAM/Au indicates the appreciable enhancement of the electrochemical behavior of PC at DNA modified onto SAM/Au compared with that modified directly at bare Au electrode. For example, the peak potential separation at bare Au and DNA/SAM/Au electrodes equal 410 and 90 mV, respectively. The separation between the anodic and cathodic peaks (Table 3S) in the case of DNA/SAM/Au was larger than that expected for a reversible one-electron process of a freely diffusing species. The present results throw the light on the interaction of PC with DNA which could be a basis for determination of the concentration of PC. In addition, it might support an idea about the curing mechanism of PC drug.

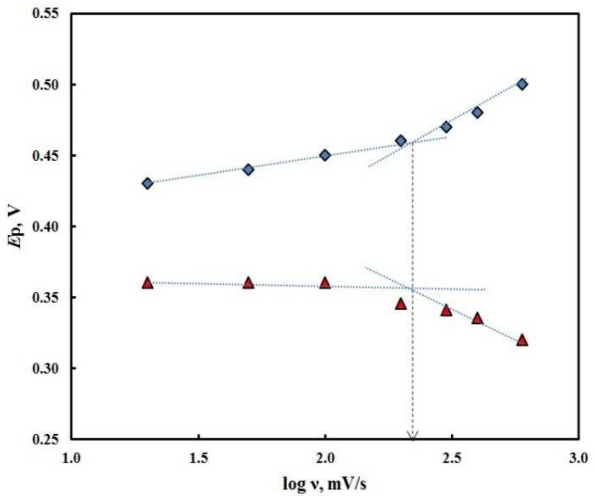

Fig. 4. Plot of log v vs. E_p for 0.053 mM paracetamol at DNA/SAM/poly–Au electrode.

Figure 1S shows the effect of the scan rate on the peak current for the oxidation and reduction of PC at DNA/SAM/Au electrode. Plot of logI_p vs. log (scan rate, ν) for 53 μM paracetamol at DNA/SAM/Au electrode is shown. A straight line obtained indicates a diffusion-controlled process. Figure 4 shows the E-logν plot for PC. From the slope, the transfer coefficient (α) was estimated using the following equation [48], and was found to equal 0.47;

$$Ep_c = E^0 - \frac{2.3RT}{\alpha\, nF}\log v \tag{2}$$

where Ep_c and E^0 are the cathodic peak potential and the equilibrium potential, respectively and n, R, T and F have their usual meaning.

Also using Tafel plot (shown in Figure 2S) which drawn from the cathodic part in cyclic voltammetry at scan rate of 20 mV/s as shown in (Figure 3, Inset). This value is consistent with the one calculated using the equation [49];

$$E_p - E_{p/2} = 48\,\text{mV}/\alpha n \ (E_p \text{ and } E_{p/2} \text{ in mV}) \tag{3}$$

where n is the number of the transferred electrons, E_p is the peak potential and $E_{p/2}$ is the half peak potential. The using of data obtained from cyclic voltammogram at scan rate of 100 mV/s, the transfer coefficient (α) was found to be 0.48.

From the effect of the scan rate on the peak current (Figure 3S), the slope was obtained and substituted in Eq. 4 in which A is the area of the electrode and C is the concentration of PC, and subsequently the diffusion coefficient, D, ($3.6\times10^{-4}\,\text{cm}^2\text{s}^{-1}$) was estimated. This is consistent with that obtained at gold nanoparticles modified electrodes [50]. This indicates the enhancement of the mass transfer of the PC and/or the electron transfer process of oxidation of PC at the electrode-solution interface [51].

Table 1. The calculated values of heterogeneous electron transfer constant (k^0) using Eq. 5.

Scan rate, V/s	Ψ	ΔEp/V	k^0	Average value ± SD
0.05	1.0	0.08	0.08395	0.069305 ± 0.015844
0.10	0.88	0.09	0.07836	
0.20	0.65	0.120	0.06683	
0.30	0.46	0.124	0.04808	

$$I_p = (2.99x10^5)nAC(\alpha nDv)^{1/2} \tag{4}$$

Nicholson method was used for calculating the heterogeneous electron transfer constant (k^0) based on its relation with a dimensionless kinetic parameter Ψ, given by the following equation [52];

$$k^0 = \Psi\left[\frac{\pi nF\nu D_0}{RT}\right]^{1/2} \tag{5}$$

Ψ values at different peak potential separation are reported [49]. Table 1 shows the heterogeneous electron transfer constant at different peak potential separation in addition to its average. The average of the heterogeneous electron transfer constant was found to equal 6.93×10^{-2}. For comparison, Giliadi method [49] was also used for the calculation of the heterogeneous electron transfer constant based on the following equation;

$$logk^0 = -0.48\alpha + 0.52 + log\left[\frac{nF\alpha V_c D_0}{2.303RT}\right]^{\frac{1}{2}} \tag{6}$$

where V_c is the critical scan rate at which the electrode reaction changes to be irreversible. This value (224 mV) was estimated from Figure 4 in which the peak potential is plotted against log-scan rate. k^0 was estimated to be 6.97×10^{-2} in consistence with the average value obtained from Nichleson method.

3.3 Electrochemical Determination of PC

Figure 4S shows the cyclic voltammograms of different PC concentrations at DNA/SAM/poly–Au electrode. As clearly shown the redox couple of PC is increasing with increasing its concentration confirming the corresponding of this redox couple to PC. Based on this, the square wave voltammograms (SWV) respond to PC and the calibration curve were obtained and shown in Figure 5. SWV has been selected as the assembly of current values is attained in a manner so that the charging current is very small. So, SWV has high immunity against changing current, and consequently its output peak is characterized by sharpness as clearly shown in Figure 5. The electrochemical re-

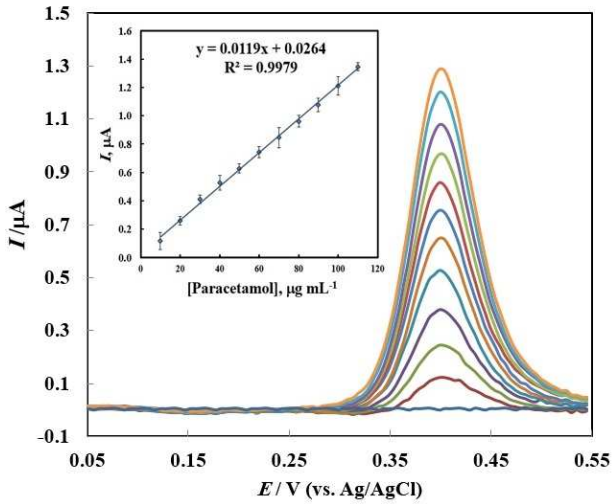

Fig. 5. SWV obtained in the presence of different concentrations of PC using scan rate of 100 mV/s.

sponse of PC at bare Au and DNA/SAM/Au by SWV is given in 5 S.

3.4 Calibration Plot

Based on the obtained above results, the use of square wave voltammetry for accurately determination of PC was benefit and valuable. SWV of PC at the modified DNA/SAM/poly–Au electrode performed at a phosphate buffer solution of pH 7 was shown in Figure 5. A clear sharp peak with an increasing in current at 0.4 V by increasing in PC concentration in the range 10.0–110.0 $\mu g\,mL^{-1}$ with a good correlation coefficient R^2 of 0.9979. The regression equation for the obtained calibration line is:

$$I, \mu A = 0.0119\ [PC], \mu g\,mL^{-1} + 0.0264$$

Both limit of detection (LOD) and limit of quantification (LOQ) were calculated based on their formulae from IUPAC's recommendations and found to be 1.18 and 5.05 $\mu g\,mL^{-1}$, respectively. For six measurements, both standard deviation (SD) and relative standard deviation (RSD) of 70 $\mu g\,mL^{-1}$ PC sample was calculated to be 0.817 $\mu g\,mL^{-1}$ and 1.52 %, respectively. To examine the usefulness of the developed method, *F*-test was calculated compared with the reference one [53] and the calculated *F* value found to be 3.59 which is less than a tabulated one 4.59 indicating that there is no significant difference between the two methods. All analytical parameters are cited in Table 2. The developed method for determination of PC was compared with previous methods of modified electrodes as cited in Table 4S [54–67]. Most recent relevant work is used here for the comparison. These data show that the detection limit was comparable with those of other electrochemical sensors [60–62,65,67]. Regarding the linear range. it is wider compared with several relevant work [60–62,65,67], and inferior compared with some others [56–59]. Most reported results are at modified carbon electrodes and few are at modified gold electrodes. In the present case DNA/SAM/Au, in addition to its usefulness in the analysis of PC, it can be used as a model for the study of the DNA-drugs interaction. The relevant results are underway. A suitable sensor for application in biological samples should fulfil some criteria, among these criteria it must differentiate the target response from possible interfering species. In the present case ascorbic acid (AA) and uric acid (UA) are the most likely interfering species. Thus, the electrochemical behavior of the PC was conducted both in the absence and presence of AA and UA. The response to PC is constant irrespective of the presence of AA and UA denoting to the immunity of the present method against AA and UA, Figure 6S.

Table 2. Analytical conditions and measurement parameters of the electroanalytical determination of PC using DNA/SAM/poly–Au electrode.

Parameters	Value
Type of buffer	Phosphate (pH 7)
Potential of measurment, V	0.4
Scan rate, $mV\,sec^{-1}$	100
Linear concentration range, $\mu g\,mL^{-1}$	10–110
Regression equation[a]	
Slope, $\mu A/\mu g\,mL^{-1}$	0.0119
Intercept, µA	0.0264
Correlation coefficient, R^2	0.9979
Standard deviation, SD (n = 6), $\mu g\,mL^{-1}$	0.817
Relative Standard deviation, RSD, %	1.52
LOD, $\mu g\,mL^{-1}$	1.18
LOQ, $\mu g\,mL^{-1}$	5.05
SD of slope	3.54×10^{-4}
SD of intercept	6.01×10^{-3}
Confidence limit[b], $\mu g\,mL^{-1}$	70 ± 1.22
F- test[c]	3.59

[a] $I(\mu A)$ = slope [PC]($\mu g\,mL^{-1}$) ± Intercept. [b]Average of six consecutive measurements. [c]Theoretical value for $F_{(6\text{-}5)}$-test at 95 % confidence limit is 4.95. Ref [53]

4 Conclusions

The present method was based on a modified gold electrode where DNA was assembled onto cysteine modified gold electrode and applied for the electrocatalysis of paracetamol. The modified electrode was characterized morphologically and electrochemically. Next, the DNA/SAM/Au electrode was used for the determination of paracetamol (PC) with the aid of SWV within a linear range of 10.0–110.0 $\mu g\,mL^{-1}$ PC. Also, the heterogeneous electron transfer constant and the diffusion coefficient for PC were estimated using Nicholson and Giliadi methods.

Acknowledgements

This paper contains the results and findings of a research project that is funded by King Abdulaziz City for Science and Technology (KAST) Grant No. 37–48.

References

[1] H. Matusiewicz, M. Ślachciński, *Microchem. J.* **2012**, *102*, 61.
[2] M. Su, W. Wei, S. Liu, *Anal. Chim. Acta* **2011**, *704*, 16.
[3] M. H. Ghanim, M. Z. Abdullah, *Talanta* **2011**, *85*, 28.
[4] H. J. Zeng, R. Yang, Q. W. Wang, J. J. Li, L. B. Qu, *Food Chem.* **2011**, *127*, 842.
[5] H. M. Qiu, Y. L. Xi, F. G. Lu, L. L. Fan, *Spectrochim. Acta Part A* **2012**, *86*, 456.
[6] H. Yu, Y. F. Tao, D. M. Chen, Y. L. Wang, L. G. Huang, D. P. Peng, M. H. Dai, Z. L. Liu, X. Wang, Z. G. Yuan, *J. Chromatogr. B* **2011**, *879*, 2653.
[7] H. Yu, Y. F. Tao, D. M. Chen, Y. H. Pan, Z. L. Liu, Y. L. Wang, L. G. Huang, M. H. Dai, D. P. Peng, X. Wang, Z. G. Yuan, *J Chromatogr. B Analyt. Technol. Biomed. Life Sci.* **2012**, *150*, 885.
[8] T. Kamei, *Procedia Eng.* **2011**, *25*, 709.
[9] H. C. Chen, Y. S. Chang, S. J. Chen, P. L. Chang, *J. Chromatogr. A* **2012**, *1230*, 123.
[10] A. Santalad, L. Zhou, F. J. Shang, D. Fitzpatrick, R. Burakham, S. Srijaranai, J. D. Glennona, J. H. T. Luong, *J. Chromatogr. A* **2010**, *1217*, 5288.
[11] H. Karimi-Maleh, A. Bananezhad, M. R. Ganjali, P. Norouzi, A. Sadrnia, *Appl. Surf. Sci.* **2018**, *441*, 55.
[12] H. Karimi-Maleh, F. T. Javazmi, N. Atar, M. L. Yola, V. K. Gupta, A. A. Ensafi, *Ind. Eng. Chem. Res.* **2015**, *54*, 3634.
[13] H. Huang, W. Bai, C. Dong, R. Guo, Z. Liu, *Biosens. Bioelectron.* **2015**, *68*, 442.
[14] B. Rezaei, M. K. Boroujeni, A. A. Ensafi, *Biosens. Bioelectron.* **2015**, *66*, 490.
[15] G. Congur, A. Erdem, F. Mese, *Bioelectrochemistry* **2015**, *102*, 21.
[16] Q. Hu, X. Deng, X. Yu, J. Kong, X. Zhang, *Biosens. Bioelectron.* **2015**, *65*, 71.
[17] S. Tajik, M. A. Taher, H. Beitollahi, M. Torkzadeh-Mahani, *Talanta* **2015**, *134*, 60.
[18] N. S. Green, M. L. Norton, *Anal. Chim. Acta* **2015**, *853*, 127.
[19] X. Ouyang, L. Luo, Y. Ding, B. Liu, D. Xu, *J. Electroanal. Chem.* **2014**, *735*, 51.
[20] P. A. Rasheed, N. Sandhyarani, *Sens. Actuators B: Chem.* **2014**, *204*, 777.
[21] T. Tian, Z. Li, E.-C. Lee, *Biosens. Bioelectron.* **2014**, *53*, 336.
[22] M. L. Yola, N. Ozaltin, *J. Electroanal. Chem.* **2011**, *653*, 56.
[23] R. T. Kachoosangi, G. G. Wildgoose, R. G. Compton, *Anal. Chim. Acta* **2008**, *618*, 54.
[24] B. J. Sanghavi, A. K. Srivastava, *Anal. Chim. Acta* **2011**, *706*, 246.
[25] B. J. Sanghavi, A. K. Srivastava, *Electrochim. Acta* **2010**, *55*, 8638.
[26] P. K. Kalambate, B. J. Sanghavi, S. P. Karna, A. K. Srivastava, *Sens. Actuators B* **2015**, *213*, 285.
[27] J. Li, J. Liu, G. Tan, J. Jiang, S. Peng, M. Deng, D. Qian, Y. Feng, Y. Liu, *Biosens. Bioelectron.* **2014**, *54*, 468.
[28] S. S. Narwade, *J. Appl. Chem.* **2014**, *7*, 46.
[29] Z. Xu, Q. Yue, Z. Zhuang, D. Xiao, *Microchim. Acta* **2009**, *164*, 387.
[30] F. S. Felix, C. M. A. Brett, L. Angnes, *J. Pharm. Biomed. Anal.* **2007**, *43*, 1622.
[31] W. T. P. Dos Santos, D. T. Gimenes, E. G. N. De Almeida, S. P. Eiras, Y. D. T. Albuquerque, E. M. Richter, *J. Braz. Chem. Soc.* **2009**, *20*, 1249.
[32] The United States Pharmacopoeia – The National Formulary – USP 23; NF-18, Twinbrook Parkway: Rockville, **1995**, p. 16.
[33] S. R. Johnson, S. D. Evans, S. W. Mahon, A. Ulman, *Supramol. Sci.* **1997**, *4*, 329.
[34] B. K. Jin, X. P. Ji, T. Nakamura, *Electrochim. Acta* **2004**, *50*, 1049.
[35] Y. Z. Fu, R. Yuan, L. Xu, Y. Q. Chai, X. Zhong, D. P. Tang, *Biochem. Eng. J.* **2005**, *23*, 37.
[36] J. W. Kang, X. N. Li, G. F. Wu, Z. H. Wang, X. Q. Lu, *Anal. Biochem.* **2007**, *364*, 165.
[37] K. Kerman, Y. Morita, Y. Takamura, M. Ozsoz, E. Tamiya, *Anal. Chim. Acta* **2004**, *510*, 169.
[38] K. Kerman, M. Saito, Y. Morita, Y. Takamura, M. Ozsoz, E. Tamiya, *Anal. Chem.* **2004**, *76*, 1877.
[39] W. S. Lu, L. Lin, L. Jiang, *Biosens. Bioelectron.* **2007**, *22*, 1101.
[40] D. J. Maxwell, J. R. Taylor, S. M. Nie, *J. Am. Chem. Soc.* **2002**, *124*, 9606.
[41] C. Y. Tsai, T. L. Chang, L. S. Kuo, P. H. Chen, *Appl. Phys. Lett.* **2006**, *89*, 203.
[42] G. Gomori, *"Methods in Enzymology"*, 1. pp. 14, Academic press, New York, **1955**.
[43] N. Norden, F. Tjerneld, *Biopolymers* **1982**, *12*, 1713.
[44] T. Bürgi, *Nanoscale* **2015**, *7*, 15553.
[45] E. Pensa, E. Cortés, G. Corthey, P. Carro, C. Vericat, M. H. Fonticelli, G. Benítez, A. A. Rubert, R. C. Salvarezza, *Acc. Chem. Res.* **2012**, *458*, 1183.
[46] S. Sahoo, A. K. Satpati, A. V. R. Reddy, *RSC Adv.* **2015**, *33*, 25794.
[47] G. D. McEwen, F. Chen, A. Zhou, *Anal. Chim. Acta* **2009**, *643*, 26.
[48] V. S. Bagotsky, *Fundamentals of Electrochemistry*, Second Edition, John Wiley & Sons, Inc. New York, **2006**.
[49] A. J. Bard, L. R. Faulkner, *Electrochemical Methods Fundamentals and Applications*, second ed. John Wiley & Sons, Inc., New York, **2001**.
[50] P. Zhang, J. Li, D. Liu, Y. Qin, Z.-X. Guo, D. Zhu, *Langmuir* **2004**, *20*, 1466.
[51] N. Yang, Q. Wan, J. Yu, *Sens. Actuators B* **2005**, *110*, 246.
[52] R. S. Nicholson, *Anal. Chem.* **1965**, *37*, 1351.
[53] E. Bayram, E. Akyilmaz, *Sens. Actuators B* **2016**, *233*, 409.
[54] H. Ghadimi, R. M. A. Tehrani, A. S. M. Ali, N. Mohamed, S. A. Ghani, *Anal. Chim. Acta* **2013**, *765*, 70.
[55] A. K. Baytak, S. Duzmen, T. Teker, M. Aslanoglu, *Mater. Sci. Eng. C* **2015**, *57*, 164.
[56] A. R. Khaskheli, J. Fischer, J. Barek, V. Vyskoci, M. I. Bhanger, *Electrochim. Acta* **2013**, *101*, 238.
[57] X. Kang, J. Wang, H. Wu, J. Liu, I. A. Aksay, Y. Lin, *Talanta* **2010**, *81*, 754.
[58] A. Yiğit, Y. Yardım, M. Çelebi, A. Levent, Z. Şentürk, *Talanta* **2016**, *158*, 21.
[59] A. M. Santos, A. Wong, A. A. Almeida, O. Fatibello-Filho, *Talanta* **2017**, *174*, 610.
[60] Y. EL Bouabi, A. Farahi, M. Achak, M. Zeroual, K. Hnini, S. El Houssame, M. Bakasse, A. Bouzidi, M. A. El Mhammedi, *J. Taiwan Inst. Chem. E.* **2016**, *66*, 33.
[61] M. Tefera, A. Geto, M. Tessema, S. Admassie, *Food Chem.* **2016**, *210*, 156.
[62] E. Bayram, E. Akyilmaz, *Sens. Actuators B* **2016**, *233*, 409.
[63] A. Wong, A. M. Santos, O. Fatibello-Filho, *Sens. Actuators B* **2018**, *255*, 2264.

[64] A. K. Baytak, S. Duzmen, T. Teker, M. Aslanoglu, *Mater. Sci. Eng. C* **2015**, *57*, 164.
[65] T. V. Gopal, T. M. Reddy, G. Venkataprasad, P. Shaikshavalli, P. Gopal, *Colloids Surf. A* **2018**, *545*, 117.
[66] S. Chitravathi, N. Munichandraiah, *J. Electroanal. Chem.* **2016**, *764*, 93.
[67] S. Bahmanzadeh, M. Noroozifar, *J. Electroanal. Chem.* **2018**, *809*, 153.

Received: March 15, 2019
Accepted: August 29, 2019
Published online on ■■, ■■

FULL PAPER

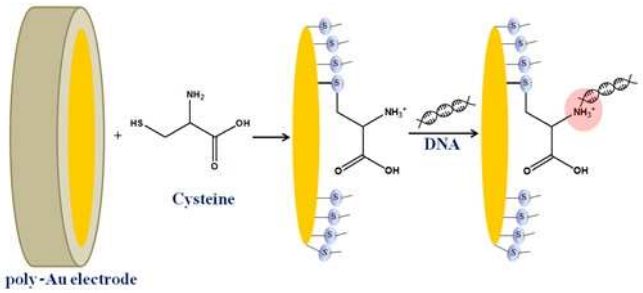

I. I. Althagafi, M. A. Kassem, M. I. Awad**